van de Moortèle, B., Reynard, B., McMillan, P. F., Wilson, M., Beck, P., Gillet, P., Jahn, S. (2007): Shock-induced transformation of olivine to a new metastable (Mg,Fe)2SiO4 polymorph in Martian meteorites. - Earth and Planetary Science Letters, 261, 3-4, 469-475,

DOI: 10.1016/j.epsl.2007.07.030.

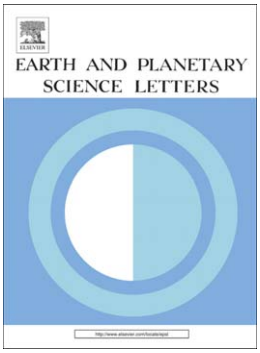

Shock-induced transformation of olivine to a new metastable $(Mg,Fe)_2SiO_4$ polymorph in Martian meteorites

Bertrand Van de Moortèle, Bruno Reynard, Paul F. McMillan, Mark Wilson, Pierre Beck, Philippe Gillet, Sandro Jahn

PII: S0012-821X(07)00452-9
DOI: doi: 10.1016/j.epsl.2007.07.030
Reference: EPSL 8820

To appear in: *Earth and Planetary Science Letters*

Received date: 3 April 2007
Revised date: 29 June 2007
Accepted date: 8 July 2007

Please cite this article as: Bertrand Van de Moortèle, Bruno Reynard, Paul F. McMillan, Mark Wilson, Pierre Beck, Philippe Gillet, Sandro Jahn, Shock-induced transformation of olivine to a new metastable $(Mg,Fe)_2SiO_4$ polymorph in Martian meteorites, *Earth and Planetary Science Letters* (2007), doi: 10.1016/j.epsl.2007.07.030

Shock-induced transformation of olivine to a new metastable $(Mg,Fe)_2SiO_4$ polymorph in Martian meteorites

Bertrand Van de Moortèle[1], Bruno Reynard[1,*], Paul F. McMillan[2,3], Mark Wilson[2], Pierre Beck[1], Philippe Gillet[1], Sandro Jahn[4]

[1]*Laboratoire de Science de la Terre, Ecole Normale Supérieure de Lyon, Université Claude Bernard Lyon 1, CNRS, 46 Allée d'Italie, 69007 Lyon, France*

[2]*Department of Chemistry and Materials Chemistry Centre, Christopher Ingold Laboratories, University College London, 20 Gordon Street, London WC1H 0AJ, UK*

[3]*Davy-Faraday Laboratory, Royal Institution of Great Britain, 21 Albemarle Street, London W1S 4BS, UK*

[4]*GeoForschungsZentrum Potsdam, Department 4, Telegrafenberg, 14473 Potsdam, Germany.*

*Corresponding author. Phone number: +33 (0) 4 72 72 81 02. Fax: xx 86 77

E-mail address: bruno.reynard@ens-lyon.fr

Introduction

Ferromagnesian olivines form the major silicate fraction of the mantle of terrestrial planets that also predominates in chondritic meteorites. The $(Mg,Fe)_2SiO_4$ phase diagram at high-P,T conditions is well established from experiments [1, 2] . The Mg_2SiO_4 end-member (forsterite; Fo) transforms first into wadsleyite-Mg_2SiO_4 and then spinel-structured ringwoodite-Mg_2SiO_4 at P = 12-22 GPa depending upon the T, before disproportionating into $MgSiO_3$ perovskite + MgO at P = 25 GPa. Fe_2SiO_4 olivine (fayalite, Fa) transforms directly into the γ-spinel polymorph at P = 6-7 GPa. High-P,T transformations of Fo,Fa olivine solid solutions lead to the high-P minerals wadsleyite or ringwoodite (i.e., β-, γ-$(Mg,Fe)_2SiO_4$). These phase transitions explain the major seismic discontinuities observed within the Earth's upper mantle and transition zone [3, 4] . Wadsleyite and ringwoodite are also documented within chondritic meteorites, where they are formed by shock metamorphism of $(Mg,Fe)_2SiO_4$ olivines. Melting is also reported to occur in certain meteorite samples. Here we studied olivine grains within the newly-described Martian meteorites NWA2737 and NWA1950 [5, 6]. Meteorite NWA1950 is a lherzolitic shergottite with a gabbroic cumulate texture. It contains 55% olivine (Fo_{66} to Fo_{75}) crystals identified by optical microscopy. NWA2737 is the second example of a chassignite meteorite, found in the Western Sahara. It is an olivine-cumulate (dunite) containing minor pyroxenes and feldspar glass. It differs slightly from Chassigny by the dark colour of its olivine crystals (Fig. 1). The olivines in NWA1950 also appear black in hand specimen.

Petrological observations

From optical and Back-Scattered Electron (BSE) microscopy, individual olivine grains in the two meteorites are clearly outlined by secondary calcite that fills grain boundaries as well as fractures within the grains. The shocked olivine crystals also contain light-coloured stripes.

Some grains exhibit sets of subperpendicular stripes, crosscut by calcite-filled fractures (Fig. 1). In BSE images, these stripes appear dark, indicating a density and/or compositional contrast with the surrounding "olivine" crystals. Micro-Raman spectra of the clear stripes exhibit sharp peaks characteristic of $(Mg,Fe)_2SiO_4$ olivine (Fig 1). The Raman spectra of the dark zones are different. Although they exhibit main features of the normal olivine spectrum, the peaks are broadened. A broad background extends from 100 to 600 cm^{-1}, and also under the high frequency region (800-1000 cm^{-1}). Such broad features could be attributed to highly disordered olivine crystals formed during the shock process. In a few crystals, a weak peak observed at 760 cm^{-1} might be assigned to formation of SiOSi linkages or highly coordinated (SiO_5, SiO_6) species as "defects" within the structure [7]. However, most grains examined did not show such a feature. Instead, the spectra showed additional broad bands at 650 and 686 cm^{-1} that cannot form part of the olivine spectrum, because the 600-800 cm^{-1} region corresponds to a well-defined gap in the vibrational density-of-states (VDOS) function [8, 9]. Weak peaks are observed at the same position in experimentally shocked olivine at 59 GPa [10]. Also, the characteristic Raman mode of olivine at 600 cm^{-1} is missing (Fig. 1). Micro-Raman mapping experiments showed that the "altered" olivine spectrum was homogeneous within both meteorite samples, both for individual grains and among different crystals. The results indicate the presence of a new phase that is structurally related to but is different from olivine, produced metastably during the shock process. We term this new orthosilicate polymorph ζ-$(Mg,Fe)_2SiO_4$ for convenience in the discussion below.

HRTEM observations

We determined the chemical composition of the dark zones and clear stripes within the shocked olivines using a combination of electron microprobe and nanoscale X-ray Energy-Dispersive analysis (ED) in the TEM studies. No difference in composition could be

established. For HRTEM studies we selected a single dark grain from NWA2737 and prepared 50-250 nm thick sections by diamond microtome (Diatome, Switzerland). The HRTEM study confirmed that the sample was entirely crystalline. Within a very few regions, selected area electron diffraction (SAED) patterns could be analysed within space group *Pbnm* with lattice parameters a = 0.4777, b = 1.026, c = 0.601 nm consistent with olivine. However, most HRTEM images indicated considerable distortion of the lattice planes, and the Fourier transformed (FT) images could no longer be indexed as olivine, although the O^{2-} anion sublattice maintained hexagonal (*hcp*) symmetry (Fig. 2). Similar results were reported for olivine crystals shocked in the laboratory and also in laser-heated Diamond Anvil Cell (DAC) experiments [11, 12]. We observed 5-30 nm metallic inclusions distributed among the shocked olivine crystals (Fig 2). EDX analysis within the TEM showed that the inclusions consisted of Fe_xNi_y alloys with their structure and composition dependent upon particle size. Asymmetric Fe-K_β and Ni-K_α peaks indicate the presence of a few amount of Co (too low to be quantify) which is consistent with Co enrichement in metal with respect to olivine [13]. The nanoparticles cause the black colour of the shocked olivines observed in hand specimen and thin section. The appearance of Fe_xNi_y in the olivine samples results metal ion reduction and migration during the shock process (well detailed in [14]). The HRTEM observations show that the olivine structure immediately surrounding the metal nanoparticles is highly ordered (Fig. 2). So far, the clear stripes observed within the black olivines do not contain metallic particles.

Molecular Dynamics simulations

We carried out Dynamics simulations (MD) to identify the nature of the new metastable Mg_2SiO_4 phase and its formation from metastably compressed olivine by shock transformation. An Anisotropic-Ion Model (AIM) is employed [15], in which induced ion

moments and short-range size and shape deformations of O^{2-} are included to quadrupolar level. The AIM is parameterised using high-level electronic structure calculations [16]. We show calculated V(P) relations for α-, β-, γ- and ζ-phases of Mg_2SiO_4 generated within a simulation box with 672 ions under constant P (variable V and cell dimensions including angles) at T=300K (Fig. 3). The new ζ-Mg_2SiO_4 polymorph has a density intermediate between α- and β-Mg_2SiO_4. It is produced in the simulation by applying a rapid P increment to metastably compressed α-Mg_2SiO_4 at P~50 GPa, mimicking the actual shock conditions. The new structure maintains an *hcp* O^{2-} sublattice and isolated SiO_4^{4-} units: it can be correlated with the olivine structure by a model proposed by Hyde et al. [17]. These authors noted that the metal cation sublattice in olivine corresponds to an alloy structure Ni_2In, with $Si(Mg,Fe)_6$ trigonal prisms linked by face-sharing to form a corrugated-prismatic structure. The γ-$(Mg,Fe)_2SiO_4$ spinel structure instead gives rise to truncated-tetrahedral $Si(Mg,Fe)_{12}$ units as found in the alloy $MgCu_2$. Both structures maintain isolated SiO_4^{4-} units and *hcp* O^{2-} packing. The ζ-Mg_2SiO_4 structure produced by MD shock compression is related to olivine by reorganisation of the metal sublattice resulting in an increase in the next-nearest-neighbour cation coordination (Fig. 4). During natural and experimental shock conditions, substantial disorder in the cation packing can result from the solid-state transformation, consistent with the HRTEM and Raman results. The AIM-MD simulations show that ζ-Mg_2SiO_4 persists metastably upon decompression to P = 1 atm. For comparison with experiment, we calculated the Vibrational Densities Of States (VDOS) and the SiO_4^{4-} stretching and bending mode contributions that dominate the Raman spectrum (Fig. 3). The VDOS are calculated both from the dynamical matrices (an instantaneous normal mode analysis) and by constructing time correlation functions which directly probe the underlying silicon-centred local modes of vibration [18]. The VDOS for the simulated ζ-Mg_2SiO_4 is similar to that of olivine but is

broadened so that features appear in the range 600-800 cm^{-1}, as observed experimentally (Fig. 1, 3).

Discussion

The conditions attained during shock are constrained by the absence of high-P wadsleyite or ringwoodite phases. The peak shock pressure in the analogous Chassigny meteorite was estimated as P~35±5 GPa from planar fractures within olivine grains, and is consistent with the observation of small (250-500 nm in size) crystals of wadsleyite and ringwoodite, indicating likely similar shock conditions for NWA2737 and NWA1950. The absence of melting indicates that T did not exceed 2500 K. Using known Fe-Ni-Mg interdiffusion coefficients for olivine we can constrain the time-temperature (t-T) conditions associated with the nanoparticle formation. The average spacing observed between nanoparticles determines a characteristic diffusion length x=50±10 nm. Using $x = (Dt)^{-1/2}$, we calculate diffusion timescales on the order of t~10 ms for T = 2100±100 K and ~1 s for T = 1600±100 K. These values correspond well with the expected duration of typical thermal events following an initial shock of this magnitude [19] .

The mechanisms of transformations between α-, β- and γ-polymorphs of $(Mg,Fe)_2SiO_4$ have been studied extensively [20-23]. A series of "spinelloid" structures exists for AB_2O_4 compounds between γ-spinel and a hypothetical structure designated the ω– or ε*- phase, formed by shifting spinel blocks relative to each other along crystal planes to create Si-O-Si linkages [17, 24]. β-Mg_2SiO_4 corresponds to one spinelloid polymorph: others have been discovered in the Ni_2SiO_4-$NiAl_2O_4$ and $NiGa_2O_4$ system, among Mg-gallogermanates and in fayalite-magnetite solid solutions [25-28]. Formation of the ω– or ε*- phase provides an intermediate step in α-(β,γ) phase transformations and leads to other spinelloid structures [17, 24]. However, the appearance of the distorted olivine phase observed following shock

compression and described above cannot be explained by the same transformation mechanism. The spinelloids are based on cubic packing of the O^{2-} sublattice, rather than the *hcp* symmetry observed here, and they contain SiOSi linkages between polymerised SiO_4 units that would give rise to strong Raman peaks both at 600-700 cm^{-1} and 950-1100 cm^{-1} [29, 30]. Instead, the Raman spectra of the shocked olivines remain characteristic of an orthosilicate structure containing isolated SiO_4^{4-} units (Fig. 1). It is thus likely that the new ζ-$(Mg,Fe)_2SiO_4$ polymorph might be present in many shocked ultrabasic rocks including meteorites, but its presence has remained undetected due to its structural and spectroscopic similarities with olivine (Fig. 3).

We calculated stable and metastable G(P) relations for α-, β-, γ- and ζ- polymorphs of Mg_2SiO_4 (G=H-TS is Gibbs' free energy; H and S are enthalpy and entropy) (Fig. 4). The AIM-MD model predicts α-β and β-γ transitions at P = 12 and 13 GPa (compared with P=9, 13 GPa from experiment after linear extrapolation to T = 0 K [1, 2]. The high kinetic barriers associated with these transitions allow olivine to be compressed metastably beyond these limits at low T [7] . The predicted ζ- polymorph becomes stabilised relative to olivine at 38 GPa. At ambient P, the free energy of the ζ-phase lies between those of α- and β-Mg_2SiO_4 so that metastable back-transformation of wadsleyite can result in formation of the ζ-polymorph. This analysis agrees with experimental studies by Raman spectroscopy and X-ray diffraction, that show formation of a new metastable structure after "gentle" heating of metastably-decompressed β-Mg_2SiO_4 recovered from high-P,T synthesis experiments [31-33].

We have thus discovered a new metastable polymorph of $(Mg,Fe)_2SiO_4$ orthosilicate within Martian meteorites in which the olivine phase was subjected to P > 35 GPa shock pressure at low T. The conditions were not sufficient to cause melting or transformation to stable high-P polymorphs. Such shock conditions are common among natural impacts [34].

References

[1] T. Katsura, H. Yamada, O. Nishikawa, M.S. Song, A. Kubo, T. Shinmei, S. Yokoshi, Y. Aizawa, T. Yoshino, M.J. Walter, E. Ito, K. Funakoshi, Olivine-wadsleyite transition in the system $(Mg,Fe)_2SiO_4$, Journal of Geophysical Research-Solid Earth 109(2004).

[2] T. Inoue, T. Irifune, Y. Higo, T. Sanehira, Y. Sueda, A. Yamada, T. Shinmei, D. Yamazaki, J. Ando, K. Funakoshi, W. Utsumi, The phase boundary between wadsleyite and ringwoodite in Mg_2SiO_4 determined by in situ X-ray diffraction, Physics and Chemistry of Minerals 33(2006) 106-114.

[3] D.J. Frost, The structure and sharpness of $(Mg,Fe)_2SiO_4$ phase transformations in the transition zone, Earth and Planetary Science Letters 216(2003) 313-328.

[4] A.E. Ringwood, Phase-transformations and their bearing on the constitution and dynamics of the mantle, Geochimica Et Cosmochimica Acta 55(1991) 2083-2110.

[5] P. Beck, J.A. Barrat, P. Gillet, M. Wadhwa, I.A. Franchi, R.C. Greenwood, M. Bohn, J. Cotten, B. Van de Moortèle, B. Reynard, Petrography and geochemistry of the chassignite Northwest Africa 2737 (NWA 2737), Geochimica Et Cosmochimica Acta 70(2006) 2127-2139.

[6] P. Gillet, J.A. Barrat, P. Beck, B. Marty, R.C. Greenwood, I.A. Franchi, M. Bohn, J. Cotten, Petrology, geochemistry, and cosmic-ray exposure age of lherzolitic shergottite Northwest Africa 1950, Meteoritics & Planetary Science 40(2005) 1175-1184.

[7] D.J. Durben, P.F. McMillan, G.H. Wolf, Raman-study of the high-pressure behavior of forsterite (Mg_2SiO_4) crystal and glass American Mineralogist 78(1993) 1143-1148.

[8] G.D. Price, S.C. Parker, M. Leslie, The lattice-dynamics and thermodynamics of the Mg_2SiO_4 polymorphs, Physics and Chemistry of Minerals 15(1987) 181-190.

[9] K.R. Rao, S.L. Chaplot, N. Choudhury, S. Ghose, J.M. Hastings, L.M. Corliss, D.L. Price, Lattice-Dynamics and Inelastic Scattering from forsterite, Mg_2SiO_4 - phonon dispersion relation, density of states and specific-heat, Physics and Chemistry of Minerals 16(1988) 83-97.

[10] S. Farrell-Turner, W.U. Reimold, M. Nieuwoudt, R.M. Erasmus, Raman spectroscopy of olivine in dunite experimentally shocked to pressures between 5 and 59 GPa, Meteoritics & Planetary Science 40(2005) 1311-1327.

[11] R. Jeanloz, Shock effects in olivine and implications for hugoniot data, Journal of Geophysical Research 85(1980) 3163-3176.

[12] F. Guyot, B. Reynard, Pressure-induced structural modifications and amorphization in olivine compounds, Chemical Geology 96(1992) 411-420.

[13] M.M. Hirschmann, M.S. Ghiorso, Activities of Nickel, Cobalt, and Manganese silicates in magmatic liquids and applications to olivine liquid and to silicate metal partitioning, Geochimica Et Cosmochimica Acta 58(1994) 4109-4126.

[14] B. Van de Moortèle, B. Reynard, P. Rochette, M. Jackson, P. Beck, P. Gillet, P.F. McMillan, C. McCammon, Shock-induced metallic iron nanoparticles in olivine-rich Martian meteorites, (in prep.).

[15] A. Aguado, L. Bernasconi, S. Jahn, P.A. Madden, Multipoles and interaction potentials in ionic materials from planewave-DFT calculations, Faraday Discussions 124(2003) 171-184.

[16] S. Jahn, P.A. Madden, Modeling Earth materials from crustal to lower mantle conditions: A transferable set of interaction potentials for the CMAS system, Physics of The Earth and Planetary Interiors 162(2007) 129-139.
[17] B.G. Hyde, T.J. White, M. Okeeffe, A.W.S. Johnson, Structures related to those of spinel and the beta-phase, and a possible mechanism for the transformation olivine-spinel, Zeitschrift Fur Kristallographie 160(1982) 53-62.
[18] E.A. Pavlatou, P.A. Madden, M. Wilson, The interpretation of vibrational spectra of ionic melts, Journal of Chemical Physics 107(1997) 10446-10457.
[19] P. Beck, P. Gillet, A. El Goresy, S. Mostefaoui, Timescales of shock processes in chondritic and martian meteorites, Nature 435(2005) 1071-1074.
[20] A.J. Brearley, D.C. Rubie, E. Ito, Mechanisms of the Transformations between the α-, β- and γ- Polymorphs of Mg_2SiO_4 at 15 Gpa, Physics and Chemistry of Minerals 18(1992) 343-358.
[21] A.J. Brearley, D.C. Rubie, Transformation mechanisms of San-Carlos olivine to $(MgFe)_2SiO_4$ beta-phase under subduction zone conditions, Physics of the Earth and Planetary Interiors 86(1994) 45-67.
[22] D.C. Rubie, A.J. Brearley, Mechanism of the Gamma-Beta-Phase Transformation of Mg_2SiO_4 at High-Temperature and Pressure, Nature 348(1990) 628-631.
[23] G.D. Price, A. Putnis, D.G.W. Smith, A Spinel to Beta-Phase Transformation Mechanism in $(Mg,Fe)_2SiO_4$, Nature 296(1982) 729-731.
[24] M. Madon, J.P. Poirier, Transmission electron microscopy observation of α, β and γ $(Mg,Fe)_2SiO_4$ in shocked meteorites: planar defects and polymorphic transitions, Physics of the Earth and Planetary Interiors 33(1983) 31-44.
[25] J. Barbier, B.G. Hyde, Spinelloid Phases in the System $MgGa_2O_4$-Mg_2GeO_4, Physics and Chemistry of Minerals 13(1986) 382-392.
[26] P.K. Davies, M. Akaogi, Phase Intergrowths in Spinelloids, Nature 305(1983) 788-790.
[27] R. Hammond, J. Barbier, Spinelloid Phases in the Nickel Gallosilicate System, Physics and Chemistry of Minerals 18(1991) 184-190.
[28] C.R. Ross, T. Armbruster, D. Canil, Crystal-Structure Refinement of a Spinelloid in the System Fe_3O_4-Fe_2SiO_4, American Mineralogist 77(1992) 507-511.
[29] P. McMillan, M. Akaogi, Raman-Spectra of β-Mg_2SiO_4 (Modified Spinel) and γ-Mg_2SiO_4 (Spinel), American Mineralogist 72(1987) 361-364.
[30] N. Choudhury, S. Ghose, C.P. Chowdhury, C.K. Loong, S.L. Chaplot, Lattice dynamics, Raman spectroscopy, and inelastic neutron scattering of orthoenstatite $Mg_2Si_2O_6$, Physical Review B 58(1998) 756-765.
[31] P.F. McMillan, M. Akaogi, R.K. Sato, B. Poe, J. Foley, Hydroxyl Groups in beta-Mg_2SiO_4, American Mineralogist 76(1991) 354-360.
[32] B. Reynard, F. Takir, F. Guyot, G.D. Gwanmesia, R.C. Liebermann, P. Gillet, High-temperature Raman spectroscopic and X-ray diffraction study of beta-Mg_2SiO_4: Insights into its high-temperature thermodynamic properties and the beta- to alpha-phase-transformation mechanism and kinetics, American Mineralogist 81(1996) 585-594.
[33] K. Tsukimura, Y. Sato-Sorenson, S. Ghose, H. Sawamoto, High-temperature single-crystal study of β-Mg_2SiO_4, EOS 69(1988) 498.
[34] D. Stoffler, K. Keil, E.R.D. Scott, Shock Metamorphism of Ordinary Chondrites, Geochimica Et Cosmochimica Acta 55(1991) 3845-3867.

Figure captions

Figure 1. Optical and electron microscopy of shocked olivine samples and Raman spectroscopy results. *(a)* Optical micrograph of a polished section of NWA2737 illustrating the unusual dark colour of the olivines in these rocks. Some clear bands are observed within the black olivine grains, with widths up to about 50 µm, oriented along two subperpendicular directions corresponding to {021} crystallographic planes. *(b)* Back-scattered electron (BSE) images show contrast between the clear bands and the majority black grains that reveals an electron density difference between the two. *(c)* Raman spectra recorded within the clear stripes correspond to pristine olivine. The spectra obtained within the dark zones resemble olivine upon first examination but they contain unusual features that can not be assigned to an olivine structure. In particular there are broad bands in the 600-700 cm^{-1} range that corresponds to a forbidden region within the VDOS of olivine crystals; also the characteristic 600 cm^{-1} peak of olivine is absent. The spectrum is reproduced throughout the majority dark crystalline material found in shocked meteorite samples NWA2737 and NWA1950, and appears constant from micro-Raman mapping studies. The spectrum likely indicates the presence of a new $(Mg,Fe)_2SiO_4$ polymorph. d) band contrast image from EBSD mapping on the same area as (b). The bright lamellae consist of well-oriented olivine (< 2° difference from point to point) and the darker majority zones to olivine-like pattern with large misorientations (5-10°) consistent with hcp structure domains.

Figure 2. High Resolution TEM images of shocked olivines within the Martian meteorite sample NWA2737. *(a)* HRTEM images of the new orthosilicate ζ-polymorph derived from $(Mg,Fe)_2SiO_4$ olivine by shock compression. The Fourier transform of the HRTEM image is readily indexed to an *hcp* lattice of O^{2-} ions and disordered cation positions with lattice

parameters *a*~0.3 nm and *c*~2*a*. Such a lattice has been proposed for high-P low-T transformations of olivine following DAC experiments[12]. *(b)* HRTEM image of a metallic Fe_xNi_y particle (15 nm diameter) contained within the shocked olivine. *(c)* Annular dark field TEM image of sub-spherical metal inclusions contained within the shocked olivine grains. *(d)* EDX spectra (normalized to the Si-K_a peak) in the precipitate and olivine matrix analysis spots (probe size 5 nm) depicted in (b). Deconvolution of analytical data yields a composition ~$Fe_{0.93}Ni_{0.07}$ for the inclusion.

Figure 3. MD results. (a) V(P) relations showing the evolution of the high pressure ζ-phase. (b) Static (0 K) energy/volume relations for the α, β, γ and ζ phases. The figure also shows the dynamic (300 K) evolution of the system energy with the arrow highlighting the location of the pressure-driven phase transition. (c) Vibrational densities of states calculated from time correlation functions constructed to reflect the vibrational modes of the SiO_4 tetrahedra. From bottom to top, the first three curves show the effect of pressure on the α-phase, whilst the upper two curves show the high and low pressure states for the ζ-phase. (d) X-ray diffraction patterns calculated from the simulated structure factors for the α-phase starting material (lower curve) and the high pressure ζ-phase (upper curve).

Figure 4. (a) Simulated free energy curves calculated as a function of pressure. The free energies are expressed relative to that of the α-phase in order to emphasize the thermodynamic phase relations. (b) Molecular dynamics snapshot of the high pressure ζ-phase shown in the *ab* plane. The Mg, Si and O atoms are shown as the red, blue and magenta circles respectively. The green box highlights the underlying unit cell.